NACA RM A9J24

NACA

RESEARCH MEMORANDUM

AERODYNAMIC STUDY OF A WING-FUSELAGE COMBINATION EMPLOYING A WING SWEPT BACK 63°.- CHARACTERISTICS AT SUPERSONIC SPEEDS OF A MODEL WITH THE WING TWISTED AND CAMBERED FOR UNIFORM LOAD

By Charles F. Hall and John C. Heitmeyer

Ames Aeronautical Laboratory
Moffett Field, Calif.

NATIONAL ADVISORY COMMITTEE
FOR AERONAUTICS
WASHINGTON

January 9, 1950
Declassified April 8, 1957

NATIONAL ADVISORY COMMITTEE FOR AERONAUTICS

RESEARCH MEMORANDUM

AERODYNAMIC STUDY OF A WING-FUSELAGE COMBINATION EMPLOYING A WING SWEPT BACK 63°.- CHARACTERISTICS AT SUPERSONIC SPEEDS OF A MODEL WITH THE WING TWISTED AND CAMBERED FOR UNIFORM LOAD

By Charles F. Hall and John C. Heitmeyer

SUMMARY

The lift, drag, and pitching-moment characteristics of a wing-fuselage combination employing a wing with the leading edge swept back 63° and cambered and twisted for a uniform load at a lift coefficient of 0.25 and a Mach number of 1.53 are presented, together with theoretical considerations leading to the development of the wing. The wind-tunnel investigation was conducted over a Mach number range from 1.2 to 1.7 and at a constant Reynolds number of 3.7 million. The experimental results are compared with values predicted by theory and obtained from other investigations.

The results show that a maximum lift-drag ratio of 8.9 and a minimum drag coefficient of 0.0145 were obtained at the design Mach number of 1.53. Between Mach numbers of 1.2 to 1.7, the lift-curve slope decreased from 0.050 to 0.044 and the neutral point shifted rearward from 57 to 64 percent of the mean aerodynamic chord. The lift-curve slope compared very well with that predicted by theory. The neutral point, however, was as much as 11 percent of the mean aerodynamic chord behind the theoretical value.

Comparison of the data with other investigations shows that the trend of the results at low supersonic Mach numbers compared well with that at high subsonic Mach numbers and comparable Reynolds number. Data obtained at a Reynolds number of 0.94 million and a Mach number of 1.53 from tests of a smaller model agreed well with those of the present investigation, indicating little Reynolds number effect in the range from 0.94 million to 3.7 million for this Mach number.

INTRODUCTION

Since the propulsive force required for an airplane in steady flight is equal to its weight divided by the lift–drag ratio of the airplane, efficient flight at supersonic speeds is possible, provided high lift–drag ratios can be obtained. In reference 1, it was shown from theoretical considerations that lift–drag ratios greater than 10 could be attained at moderate supersonic speeds by using a thin swept wing of high aspect ratio lying within the Mach cone from the apex of the leading edges. To determine experimentally the characteristics of such wing plan forms, an investigation has been undertaken at Ames Aeronautical Laboratory. This investigation is concerned primarily with wing–fuselage combinations having wings with leading edges swept back 63°. The facilities employed afford wide ranges of Mach number and of Reynolds number.

The results of the first phase of the investigation, concerned with an untwisted and uncambered wing, were reported in references 2, 3, and 4. In reference 2, the results of tests at a Mach number of 1.53 indicated that a maximum lift–drag ratio substantially less than that predicted by theory was obtained. The failure of the experimental lift–drag ratio to agree with theory was attributed primarily to the inability of the uncambered wing sections to carry the required lift without excessive drag. Study of unpublished section data from the Ames 1– by 3–1/2–foot high–speed wind tunnel indicates that the lift may be carried with low drag if the airfoil section is cambered.

Solutions for the shape of the wing surface required to support a uniform load have been derived in reference 1. These solutions were used to develop the camber of the airfoil sections and to provide a guide for twisting the swept wing to give uniform load at a lift coefficient of 0.25 at a Mach number of 1.53.

A small–scale wing incorporating this twist and camber was tested in the Ames 1– by 3–foot supersonic wind tunnel at a Mach number of 1.53 (reference 5). The data did not show the improvement in lift–drag ratio that was expected, a result which was believed due to separation of the laminar boundary layer at the low Reynolds number of the investigation. The experiments of the present report were undertaken, therefore, to determine the characteristics of the twisted and cambered wing at supersonic speeds and at a Reynolds number more nearly comparable to flight Reynolds numbers at high altitudes. In addition to these experimental results, the present report also contains a discussion of the theoretical considerations leading to the development of the twisted and cambered swept–back wing.

The results of tests of the twisted and cambered wing with the leading edge swept back 63° at Reynolds numbers comparable to flight in a high subsonic speed wind tunnel are presented in reference 6.

NOTATION

b	span, feet
c	chord parallel to plane of symmetry, feet
$\bar{c}$	mean aerodynamic chord $\left(\frac{\int_0^{b/2} c^2 dy}{\int_0^{b/2} c\, dy} \right)$, feet
C_L	lift coefficient
$C_{L_{D_{min}}}$	lift coefficient for minimum drag coefficient
C_{L_α}	rate of increase of lift coefficient with angle of attack at zero lift, per radian unless specified otherwise
C_m	pitching-moment coefficient, referred to quarter-chord point of mean aerodynamic chord
C_D	drag coefficient
$C_{D_{min}}$	minimum drag coefficient
dC_m/dC_L	rate of change of pitching-moment coefficient with lift coefficient at zero lift
$\Delta C_D/\Delta C_L^2$	drag-rise factor
L/D	lift drag ratio
M	Mach number
m	β times cot Λ
R	Reynolds number
T	leading-edge thrust, pounds

u all components of perturbation velocity in x direction which go to infinity at leading edge, feet per second

x,y,z Cartesian coordinates for wing plan form in directions longitudinal, lateral, and normal to plan form, respectively, feet

α angle of attack measured with respect to fuselage axis of symmetry, degrees

$\alpha_{C_L = 0}$ angle of attack at zero lift, degrees

β $\sqrt{M^2 - 1}$

Λ angle of sweepback of leading edge, degrees

ρ density, slugs per cubic foot

THEORY

The theoretical treatment of many three-dimensional wing problems is based upon a linearization of the equations of motion made possible by the assumption that the disturbance velocities are small. Such treatments are justified because the assumption is consistent with the requirements of an efficient aircraft. As a result of the linearization, the principle of superposition of solutions applies.

Since the principle of superposition applies, a three-dimensional wing problem involving complex boundary conditions may be solved by reducing it to a series of problems of less complex boundary conditions, the solutions for which are known or can be readily found. The theoretical treatment in the present report is so developed.

Design of Wing

Wing plan form.- The advantages of sweepback for wings designed for supersonic flight have been known for some time. It was pointed out in reference 7 that the pressure distribution on a wing of infinite aspect ratio is determined essentially by the component of velocity normal to

the leading edge. Thus, for an infinite wing with its leading edge swept behind the Mach lines a subsonic-type pressure distribution occurs over the airfoil section and the attachment of plane waves is avoided. The drag due to lift which occurs for unswept wings is also eliminated, since the theory shows that, for the swept infinite wing, the drag due to the lifting pressure acting normal to the chord plane is exactly compensated by the upstream force due to the suction pressure at the leading edge.

The research of reference 7, however, did not show quantitatively the effects of aspect ratio on the lift and drag of wings swept behind the Mach line at supersonic speeds, nor did it indicate the amount of sweepback required for efficient flight. Further theoretical research was performed (reference 1) to determine wing plan forms suitable for flight at supersonic speeds. In this work, wings of various aspect ratios, taper ratios, thickness, and sweepback were investigated using existing wing structure criteria to obtain feasible wing aspect ratios and taper ratios. This investigation indicated that, for a design Mach number of 1.53, the optimum wing plan form was one having the leading edges swept back 63°, an aspect ratio of 3.5, and a taper ratio of 0.25. It is interesting to note, also, that for the Mach number range from 1.15 to 2.0 the theory indicated that the optimum sweep varied only from 53° to 70°.

Twist and camber.- It was also shown in reference 1 that flat wings of the afore-mentioned plan form developed a high section loading at the tips and that the chordwise distribution of load gave very high peak pressures near the leading edge. Such load concentrations are undesirable from both the aerodynamic and structural points of view. To avoid this condition the solution for the camber and twist of a swept wing designed to support a uniform load was developed in reference 1.

Examination of this solution shows that, for wings with leading and trailing edges swept behind the Mach line, at a distance from the center section the section contour for a uniform-load wing resembles that of the constant load mean line (a=1) used for subsonic airfoils. At the center section, however, the solution shows an infinite slope. This condition is impossible of fulfillment on an actual wing but it is believed not to invalidate the theory because of the following reasons:

1. A short distance from the center, the contour acquires a reasonable slope.

2. The fuselage usually encloses that part of the wing for which the theory indicates excessive twist.

It should be noted that the solution for a uniformly loaded wing given by reference 1 can be extended to many other types of spanwise and chordwise load distributions. Research on this subject has shown that the chordwise loading may be easily changed from the a=1 type to the a=0.5 type, both of which are familiar to designers. The span loading can be made rectangular, elliptical, triangular, or trapezoidal.

Thickness.– As yet there is no theory from which the optimum thickness distribution for a swept–back wing can be obtained. It seems logical to suppose from simple sweep theory, however, that the same criteria used to select the thickness distribution for a wing designed for high subsonic speeds would be used for a swept–back wing also. The thickness should be as small as possible consistent with strength requirements. The thickness distribution should be such as to produce no large adverse pressure gradients which would promote separation and to have a well–rounded leading edge to delay leading–edge separation and permit the attainment of large leading–edge suction at lift coefficients other than design. An NACA 64A005 airfoil section was selected as the thickness distribution for streamwise sections of the wing of the present investigation.

Calculation of the Wing Characteristics

The effects of angle of attack, twist and camber, thickness, and elastic deformation due to load on the aerodynamic characteristics of the wing are treated separately.

Angle of attack.– Since in the linear theory the wing characteristics which are functions of the angle of attack are determined solely by the wing plan form, it is permissible to consider the wing as a flat plate having an identical plan form. The aerodynamic characteristics of such wings have been treated extensively in references 8 and 9. The methods of these references were used to determine lift–curve slope, slope of the pitching–moment curve, and the drag due to the lift obtained by increasing angle of attack.

The supersonic theory shows that the drag due to lifting pressures is proportional to the square of the lift, and all other forces comprising the drag are either constant or directly proportional to the lift. It is thus possible to express the relationship between lift and drag coefficients as a parabolic equation as follows:[1]

$$C_D = C_{D_{min}} + \left(\frac{\Delta C_D}{\Delta C_L{}^2}\right)\left(C_L - C_{L_{D_{min}}}\right)^2 \qquad (1)$$

The quantity $\Delta C_D/\Delta C_L{}^2$, which is the factor of proportionality between the drag coefficient due to the lift produced by angle–of–attack change and the square of the lift coefficient, has come to be known as the drag–rise factor. The quantity is useful since the complete description of the drag polar is obtained by stating its value and the lift and drag coefficients at minimum drag.

[1]A constant term and the terms proportional to lift coefficient are contained in the second term of the right–hand side of the equation (1).

The drag-rise factor is composed of two terms: one due to the leading-edge suction force, and the other due to the component in the drag direction of the pressure force acting normal to the surface of the flat wing. The concept of a leading-edge suction force came about originally in subsonic thin-airfoil theory. (See reference 10.) This suction force was shown to exist by a mathematical treatment of the singularity in the flow at the wing leading edge. Its magnitude was found to be exactly equal to the drag component of the pressure forces acting normal to the wing surface so that the airfoil experienced no net drag in an inviscid fluid. A similar mathematical treatment of the flow singularity which occurs at the leading edge of a lifting flat wing swept behind the Mach lines at supersonic speeds also shows the existence of a suction force. At supersonic speeds, however, the leading-edge suction for a swept-back wing of finite aspect ratio is not great enough to compensate completely for the normal force drag so that, when all drag forces for the entire wing are summed up, there is a net wave drag due to lift. Since the leading-edge suction force per unit span varies linearly with spanwise position for a swept-back wing, vanishing at the plane of symmetry, the aspect ratio is an important parameter insofar as drag is concerned, the effect of aspect ratio being qualitatively similar to that at subsonic speeds.

Twist and camber.- The twist and camber of an airfoil determine the angle of attack and pitching moment at zero lift and influence the lift and drag at minimum drag. These wing characteristics can be determined theoretically only at the design Mach number, since at present there is no theory which shows quantitatively the effects of Mach number variation on the loading due to camber and twist and, therefore, on the lift and drag characteristics of a twisted and cambered airfoil. The effects of twist and camber on the theoretical characteristics of the wing of the present investigation, therefore, are not given.

Thickness.- The theory shows that thickness affects only the minimum drag coefficient. No calculations were made for the effects of thickness, therefore, because the drag due to thickness for a swept-back wing with rounded leading edges at present has not been determined theoretically.

An estimate of the thickness drag may be obtained by substituting biconvex or double-wedge sections for the round nose section. Another possible method of determining the thickness drag is based upon the work of reference 11. In this work the nonlifting pressure distribution for a triangular wing having sections resembling conventional subsonic sections was obtained and the thickness drag determined.

Elastic deformation.- For a swept-back wing the bending deformation of the wing due to aerodynamic loads results in a negative twist, reducing section angles of attack at the tip. Since this twist is proportional to the load, it varies with angle of attack. The change in load at the outboard sections of the wing with increasing angle of attack is therefore less for an elastic than for a rigid wing, resulting in a smaller lift-curve slope and a more forward position of the center of pressure.

The effects of elasticity must be considered, therefore, in determining the aerodynamic characteristics of a swept-back wing. In the present report the effects of elasticity as given by reference 12 have been considered in calculating the theoretical characteristics of the model rather than in correcting the experimental results. Hence, both the theoretical and experimental results presented herein contain the effects of elastic deformation of the model.

The effects of elasticity on drag are not treated in reference 12. It is possible, however, to calculate the drag of the elastic wing by integrating the product of the local angle of attack times the section lifts due to the angle of attack and due to the elastic deformation of the wing, as determined in reference 12. The leading-edge suction for the elastic wing was determined from the following expression, a form of which was derived in reference 13:

$$\frac{dT}{dy} = \frac{\beta\pi\rho\sqrt{1-m^2}}{m^2} u^2(mx-\beta y) \qquad (2)$$

In the calculations of the effects of elasticity, the experimentally determined angle of twist of the wing (0.23° per degree angle of attack) was used. The results of the calculation for the model wing are shown in figure 1. The data indicate that the elastic deformation effects are sizable.

EXPERIMENT

Description of Apparatus

Wind tunnel.- The experimental investigation reported herein was conducted in the Ames 6- by 6-foot supersonic wind tunnel which is described in reference 14. The Mach number in this tunnel is continuously variable from 1.2 to 2.0, although at the present time the maximum Mach number is limited to 1.7 because of strength and vibration limitations of the model support.

Model.- The model used for the present investigation, identical to that used in the tests of reference 15, is shown mounted in the wind tunnel in figure 2. A plan view of the model and dimensions are given in figure 3. The distributions of camber and twist along the wing span, shown in figure 4, have been modified from that determined by the theory to reduce the large twist at the root indicated by the theory and to account for the twist due to elastic deformation of the wing when carrying the load obtained at a lift coefficient of 0.25, a Mach number of 1.53, and a dynamic pressure of 1100 pounds per square foot.

Selection of the fuselage shape for the investigation was based upon theoretical considerations (reference 16) which showed the shape to have a minimum wave drag for a given volume and length of body. The fineness

ratio of the fuselage was 12.5. The aft 21 percent of the fuselage, shown dotted in figure 3, was removed to allow the model to be supported by the sting.

The model was constructed of steel and the surface was painted and sanded to a smooth finish.

Balance.- The aerodynamic forces and moments were measured by a four-component strain-gage balance in the body of the model. The balance is so designed that each force or moment component is measured by one strain gage only and each gage is supported by ball bearings so that interaction between the various gages is eliminated. The forces and moments are measured by galvanometers calibrated by applying known loads on the model.

Range of Test Variables

Lift, drag, pitching-moment, and base-pressure measurements were made through a Mach number range from 1.2 to 1.7. The corresponding dynamic pressure range was from approximately 740 to 810 pounds per square foot. The angle of attack was varied from 0° to 10° in approximately $1-1/4^\circ$ increments. The Reynolds number was held constant and equal to 3.7 million.

Effects of Stream Characteristics

Of primary importance in obtaining reliable results from a wind-tunnel investigation is a knowledge of the characteristics of the wind-tunnel stream. The flow characteristics in the test section of the Ames 6- by 6-foot supersonic wind tunnel have been obtained from extensive surveys and were discussed in reference 14. The stream characteristics and their effects on the wind-tunnel results are noted only briefly here.

The surveys showed that at some Mach numbers there is some inclination and curvature of the stream in the vertical plane, but no curvature or cross flow in the horizontal plane. To minimize the effects of these stream irregularities on the longitudinal characteristics of the wing-fuselage combination, the model was mounted with the wing in the vertical plane as recommended in reference 14. Although this method of mounting the model eliminates induced camber effects on the wing, it produces a slight yaw angle due to the stream curvature which varies along the span of the wing. The effects of these yaw angles are believed to be negligible, however, since unpublished results from an investigation in the 6- by 6-foot wind tunnel of the lateral characteristics of the wing-fuselage combination of the present investigation show that the longitudinal characteristics were unaffected by small angles of yaw.

The stream surveys also showed a variation of Mach number in the vertical direction which caused the free-stream Mach number at the wing tips for some test conditions to be as much as 4 percent different from that at the wing root. (The free-stream Mach number at the wing root was taken as the over-all stream Mach number in the present investigation.) However, the variation of free-stream Mach number across one wing panel was approximately equal but of opposite sign to that across the other wing panel. Thus with respect to longitudinal characteristics, the effect of the Mach number variation across one wing panel tends to compensate for that across the other panel.

A variation in the static pressure along the tunnel axis also was shown by the stream surveys. Along a length of 60 inches the variation was as much as 4 percent of the dynamic pressure at some Mach numbers. The resulting pressure gradient acts on the model fuselage to produce a force in the longitudinal direction which was calculated in the manner discussed later.

Reduction of Data

The force and moment coefficients presented in this report are based upon the complete projected wing which includes the area formed by extending the leading and trailing edges to the plane of symmetry. The pitching-moment coefficient is based upon the mean aerodynamic chord of the complete projected wing and the center of moment is taken as the quarter chord of the mean aerodynamic chord. The Reynolds number is also based upon the mean aerodynamic chord.

The dynamic pressure was calculated from the total pressure and Mach number of the stream. The free-stream Mach number was that measured at the intersection of the wind-tunnel axis and the test-section center line and in general approximated the mean of the Mach number values determined throughout the test section during the calibration.

The strain-gage balance, located inside the fuselage of the model, measured the normal and chord forces. These forces were resolved into the lift and drag forces.

Corrections to Data

The longitudinal buoyant force caused by the axial static pressure variation in the test section, mentioned previously, was calculated by integrating graphically the product of the static pressure and the change in cross-section area of the fuselage along its length. The measured drag was corrected by this longitudinal force, which, converted to a coefficient, amounted to as much as 0.0007 at a Mach number of 1.3.

The determination of the base drag of the fuselage is of primary importance in obtaining valid drag data from model tests. In the present

investigation the aft portion of the body was removed to accommodate the sting support. If this were not necessary, the fuselage would be lengthened as indicated by the dotted lines of figure 3 to that point at which the resultant base diameter was equal to that required by the jet. The pressure on this additional part of the fuselage has been determined by the method of characteristics and is nearly free-stream static pressure. The pressure on the modified base area also would be approximately free-stream static pressure if it were assumed that a jet was issuing from the base. The effect of these pressures on the additional part of the fuselage is approximately the same, therefore, as the effect of free-stream static pressure on the base of the present model. Thus, in the present investigation, the base drag was made equal to the base area times the free-stream static pressure, and a correction was made to the measured drag to account for the difference between this base drag and the measured base drag.

The effects of support interference on the wind-tunnel results must also be considered in obtaining correct results. In reference 17, it was shown that, for the ratio of sting diameter to base diameter used in the present investigation, this effect was confined to a change in base pressure. Thus the effect of support interference was taken into account in making the base drag correction discussed in the previous paragraph.

Precision of Data

The accuracy of the experimental data can be determined by considering the uncertainty in the factors which are involved in the determination of these data. The uncertainty in any factor was taken as one of the following:

1. The least reading of the instrument for quantities that were steady during the investigation

2. The magnitude of the fluctuation for quantities that were unsteady during the investigation

3. The variation from the mean for quantities which could be repeated under similar fixed conditions

Force and moment measurements.- As mentioned previously, the forces on the model were measured on galvanometers calibrated by applying known loads on the model. The least reading of these galvanometers caused an uncertainty of less than 1 percent in the force measurements. The balance calibration factors for lift, drag, and pitching moment varied as much as ± 0.3, ± 0.7, and ± 0.4 percent, respectively, over a period of several months. These calibration factors were unaffected by temperature or pressure variation. In addition, the calibration data showed there was no interaction between the various forces and that the balance and galvanometer were reasonably free of friction.

Angle measurements.– The angle of attack for the model was determined by measuring the angle of attack with the tunnel stopped and adding the incremental angle due to deflection of the sting and strain gage under aerodynamic load. The static angle of attack was determined by measuring the horizontal displacement of the nose of the fuselage with respect to its base. The accuracy of these measurements were ±1/64 inch, which produced an uncertainty of 0.04° in the static angle of attack. The uncertainty in the incremental angle due to aerodynamic loads was 8 times 10^{-5} and 6 times 10^{-4}, degree per pound lift and per pound–foot moment, respectively.

Pressure measurements.– Pressures were measured with manometers using either tetrabromoethane (specific gravity = 2.96) or mercury (specific gravity = 13.6). Tetrabromoethane was used in measuring the base pressure and the height of the fluid fluctuated as much as ±0.2 centimeters during a reading, causing an uncertainty of as much as ±3 percent in the measured base drag. A mercury–filled manometer was used to measure the total pressure, the least reading of 0.1 centimeter, causing an uncertainty of approximately 0.2 percent. The dynamic pressure was calculated using the total pressure and free–stream Mach number, the accuracy of the latter being ±0.01. Since the wind–tunnel air humidity was always below 0.0003 pound of water per pound of air, the effect of humidity on dynamic pressure was negligible.

The Reynolds number was calculated using the free–stream Mach number and the measured total pressure and temperature. The average Reynolds number for all the runs was 3.69 million with a maximum variation of ±0.03 million.

Final uncertainty.– The final uncertainty in the data was taken as the square root of the sum of the squares of the uncertainties in the factors making up the various results. The following table lists these uncertainties:

Quantity	Uncertainty	
	$\alpha = 0°$	$\alpha = 10°$
Lift coefficient	±0.0005	±0.003
Drag coefficient	±.0002	±.001
Pitching–moment coefficient	±.0002	±.0013
Angle of attack	±.04°	±.12°
Mach number	±.01	±.01
Reynolds number	±.03 million	±.03 million

DISCUSSION

General Characteristics

The lift coefficient as a function of angle of attack and the pitching-moment coefficient, drag coefficient, and lift-drag ratio as functions of the lift coefficient are shown in figures 5 to 8. The data indicate a linear variation of lift coefficient with angle of attack and of pitching-moment coefficient with lift coefficient up to a lift coefficient of approximately 0.2 throughout the Mach number range of the tests. In general, above a lift coefficient of 0.2, both the rate of increase of lift coefficient with angle of attack and the static stability, as determined by the slope of the pitching-moment curve, decreased with increasing lift coefficient. Above a lift coefficient of approximately 0.4 the model was unstable about the quarter chord of the mean aerodynamic chord. The afore-mentioned lift and pitching-moment characteristics of the wing above a lift coefficient of 0.2 are believed to be the result of flow separation on the outboard sections of the wing near the trailing edge. This conclusion was substantiated by the results of liquid-film studies of the flow over the wing at a Mach number of 1.53 and an angle of attack of 5.3°. Observations of tufts also indicated flow separation in the manner defined in reference 18 near the trailing edge and outboard of 50 percent of the semispan of the wing for lift coefficients above approximately 0.2 and throughout the Mach number range. The tufts were glued to the wing aft of 50 percent of the wing chord. Above approximately a lift coefficient of 0.2 the tufts near the trailing edge vibrated violently at first and then, with a slight increase in angle of attack, showed the boundary-layer flow to be in the spanwise direction.

The effect of flow separation was also indicated by the drag results. The data showed that above a lift coefficient of approximately 0.2, the increase of drag coefficient with the square of the lift coefficient was greater than at the lower lift coefficients. A typical example of this characteristic is shown in figure 7 by comparing the drag polar for a Mach number of 1.2 with the parabola having a drag-rise factor equal to that of the polar at a lift coefficient less than 0.2.

The data of figure 8 show that the maximum lift-drag ratio decreased with increasing Mach number, but the range of lift coefficient in which lift-drag ratios near the maximum were obtained increased slightly with Mach number. Thus lift-drag ratios within 10 percent of the maximum were obtained over a lift-coefficient range of 0.17 at a Mach number of 1.53 but only a range of 0.13 at a Mach number of 1.20.

Effects of Mach Number

As was previously noted, the effects of the elastic deformation of the wing under aerodynamic load have been considered in computing the

theoretical results which are compared with the experimental results in this section. These effects are important in the design of aircraft with large sweep, particularly if the dynamic pressures are high and must be considered in the estimation of full-scale aerodynamic characteristics from wind-tunnel results.

Lift-curve slope.- The data of figure 9 show that the lift-curve slope decreased from 0.50 to 0.044 as the Mach number increased from 1.2 to 1.7. These values compare well with those values of 0.048 and 0.047 predicted by theory for the same Mach number range. The differences between the experimental and theoretical results over the Mach number range can be correlated with the results of the pressure-distribution measurements on this wing reported in reference 15. These chordwise pressure measurements were integrated graphically to determine the distribution across the span of the loading due to angle of attack. The results showed that at the lower Mach numbers the spanwise loading was higher than predicted by theory, particularly at sections outboard of approximately 50 percent of the semispan, but with increasing Mach number became less than predicted by the theory. Thus, it was principally the difference in loading on the outboard sections of the wing over the Mach number range which accounted for the discrepancy between the theoretical and experimental lift-curve slopes.

Angle of zero lift.- The angle of zero lift is a function of both the lift due to angle of attack and the lift due to camber and twist. Since the latter factor was not determined theoretically, no theoretical values for the angle of zero lift are shown. The experimental results (fig. 9) show that the angle of zero lift increased from 0.6° at a Mach number of 1.2 to 1.0° at a Mach number of 1.7. This trend conforms with the expected effect of Mach number on the lift due to camber and twist. This effect is masked somewhat in the experimental data, however, by the fact that the lift-curve slope is decreasing with increasing Mach number. A decrease in lift-curve slope would tend to decrease the angle of zero lift for a twisted and cambered wing.

Position of neutral point.- The data of figure 10 show that the neutral point[2] shifted rearward from 57 to 64 percent of the mean aerodynamic chord as the Mach number increased from 1.2 to 1.7. The position of the neutral point did not agree too well with that predicted by theory, being as much as 11 percent of the mean aerodynamic chord aft of the theoretical value. In addition, the rearward movement of the neutral point with increasing Mach number was somewhat less than predicted by theory. As noted previously, the results of the pressure-distribution measurements of reference 15 can be used to explain in part these discrepancies. At the low Mach numbers the experimentally determined load, particularly over the outboard sections of the wing, was higher than the

[2]The neutral point was determined from the slope of the pitching-moment curve at zero lift.

theoretical load and therefore the experimental neutral point was farther aft than that predicted by the theory. With increasing Mach number the experimental loading decreased with respect to the theoretical loading, the largest change occurring outboard of approximately 50 percent of the wing semispan. This change in loading caused the neutral point determined from the pressure measurements on the wing to be forward of that determined from theory at the higher Mach numbers, a result opposite to that obtained from the force tests. It appears, therefore, that part of the discrepancy was due to another effect which increased with Mach number and tended to make the experimentally determined neutral point aft of that determined by theory. It is believed that this additional part of the discrepancies can be attributed to the fact that the theory does not consider the effects of the wing–fuselage interference. Calculations based on reference 19 account for only a minor portion of the difference between the theoretical and experimental data of figure 10. It appears that a major portion of the effect of the wing–fuselage interference on the position of the neutral point comes about because the portion of the wing lift carried by the fuselage has its center of pressure farther back on the fuselage than indicated by an essentially subsonic theory (reference 19). This rearward location of the "carry–over" lift is due to the fact that the wing influences the fuselage pressure distribution only within the Mach cones from the intersections of the wing leading edge and fuselage. Theoretical studies of this effect are indicated since the change in stability resulting therefrom is of significant magnitude.

Pitching–moment coefficient at zero lift.– The pitching–moment coefficient at zero lift is a function of the centers of lift due to angle of attack and of lift due to camber and twist. No theoretical results are shown because the latter term cannot be treated. The experimental results (fig. 6) show that the pitching–moment coefficient at zero lift increased from −0.011 at a Mach number of 1.2 to −0.001 at a Mach number of 1.7. This characteristic would be expected from the effects of Mach number on the lift due to camber and twist. However, the rearward movement of the neutral point would also be expected to cause an increase in the pitching moment at zero lift for a cambered and twisted wing. The experimental results do not indicate clearly the effects of Mach number on the position of the center of load due to camber and twist.

Drag–rise factor.– In figure 11, the experimental drag–rise factor (previously noted as a concept arising from the linear theory) is compared with that predicted by theory, both assuming full attainment of the theoretical leading–edge suction force and assuming no leading–edge suction force, the value for the latter case being equal to the reciprocal of the lift–curve slope. The experimental drag–rise factor was determined from the equation of a parabola which most closely approximated the drag curves of figure 7 between 0° and 5° angle of attack. The data indicate that the experimental drag–rise factor was between the theoretical result for complete realization of the theoretical leading–edge suction force and that

for no leading-edge suction force, although somewhat closer to the latter. This result does not indicate that the experimental leading-edge suction force was less than that predicted by theory, however. The theoretical drag-rise factor is a function only of the drag component of the force due to the lifting pressures and the leading-edge suction force and does not consider possible variation with lift coefficient of friction drag and its effects. It is possible, therefore, that much of the increase in the drag-rise factor above the optimum theoretical value could be due to an incomplete recovery of the pressure near the trailing edge of the wing due to viscous effects.

Maximum lift-drag ratio and minimum drag coefficient.- In figure 12, the effects of Mach number on the maximum lift-drag ratio are shown. The results indicate a decrease in maximum lift-drag ratio from 12.2 to 7.9 as Mach number was increased from 1.2 to 1.7. For the present investigation this decrease in maximum lift-drag ratio was caused mainly by the increase in minimum drag coefficient from 0.0115 to 0.0155 (fig. 13). The decrease in lift coefficient for minimum drag from 0.060 to 0.025 (fig. 7) and the increase in drag-rise factor from 0.26 to 0.33 (fig. 11) caused the decrease in maximum lift-drag ratio to a smaller degree.

The increase in minimum drag coefficient is believed to be caused mainly by the increase in the pressure drag due to thickness. Based upon the theoretical results for a constant-chord wing having a biconvex section and a tapered wing having a double-wedge section, it is estimated that this increase was approximately 0.0029, or 73 percent of the total increase in minimum drag. The remainder of the increase in minimum drag coefficient is caused probably by the effects of Mach number on the loading due to camber and twist. It seems, therefore, that the effects of Mach number on the load due to camber and twist also have an influence on the variation of maximum lift-drag ratio with Mach number and that there is need for a quantitative study of these effects.

Comparison of Results With Those From Other Investigations

As previously noted, an extensive program for investigating the characteristics of a 63° swept-back wing has been conducted by several of the facilities at the Ames Aeronautical Laboratory. The results of the present report will be compared with those from the other investigations to point out possible discrepancies and to discuss various factors which may affect the results from each investigation differently.

Results from Ames 12-foot pressure wind tunnel.- A model having the same geometric characteristics as the model of the present investigation was tested in the Ames 12-foot pressure wind tunnel up to a Mach number of 0.93 at a Reynolds number of 2.0 million. In general, the trend of the data at high subsonic speeds conforms well with that of the present investigation at low supersonic speeds (figs. 9 to 13).

Since it is unlikely that irregularities would exist in the characteristics of a highly swept wing between Mach numbers of 0.93 and 1.20 (see reference 20 for investigations of swept wings in the transonic region), the lack of data in this region is not considered serious and these two sets of data therefore define well the characteristics of the 63° swept-back wing through the complete Mach number range up to 1.7.

The results of both investigations show that with increasing Mach number the lift-curve slope (fig. 9) increased in the subsonic range, reached a maximum between Mach numbers of 0.93 and 1.2, and decreased in the supersonic ranges. The neutral point (fig. 10) moved rearward with increasing Mach number throughout the range of both investigations, shifting from 41 percent to 64 percent of the mean aerodynamic chord with increasing Mach number from 0.4 to 1.7. The data indicate that the largest rearward shift, approximately 11 percent of the mean aerodynamic chord, occurred between Mach numbers of 0.93 and 1.20. The results of figure 11 indicate that, with increasing Mach number, the drag-rise factor was constant up to a Mach number of 0.7 and increased steadily over the remainder of the Mach number range. The maximum lift-drag ratio (fig. 12) decreased with increasing Mach number throughout the range of both investigations. The value of maximum lift-drag ratio at a Mach number of 1.2 appears to be slightly high, however, by comparison with the results at the other Mach numbers. Also, the value of the minimum drag coefficient at a Mach number of 1.2 (fig. 13) may be slightly low by comparison with the results at the other Mach numbers. The cause of these discrepancies is not known. Erroneous corrections for the longitudinal buoyant force on the body or determination of the base drag apparently are not the cause, since the results of body-alone tests using identical values for these corrections appear quite reasonable. The discrepancies probably are the result of unknown stream disturbances at a Mach number of 1.2 affecting the flow over the wing.

It should be mentioned that the effect of the elastic deformation of the wing due to aerodynamic loads on the data obtained in the 12-foot wind tunnel at high subsonic Mach numbers was roughly one-half the elastic deformation effects experienced in the 6- by 6-foot wind-tunnel tests.[3] With effects of elasticity on the data from the 12-foot wind tunnel comparable to those on the 6- by 6-foot wind-tunnel tests, the lift-curve slope (fig. 9) would be roughly 5 percent less and the neutral point (fig. 10) 1 to 2 percent of the mean aerodynamic chord farther forward than indicated by that investigation. The differences in the effects of elastic deformation would probably have no appreciable effect on the relative magnitudes of the drag characteristics. (See figs. 11 to 13.)

[3] In reference 12, it was shown that the effects of elastic deformation on the characteristics of a wing are primarily a function of dynamic pressure. The dynamic pressure at 0.9 Mach number of the investigation in the 12-foot wind tunnel was approximately one-half that of the present investigation.

Results from Ames 1- by 3-foot supersonic wind tunnel.- The characteristics of a model geometrically similar to that of the present report were investigated in the Ames 1- by 3-foot supersonic wind tunnel at a Mach number of 1.53 and a Reynolds number of 0.94 million.[4] Comparison of the data with those of the present investigation indicates that the effects of Reynolds number on the 63° swept-back wing in the range of Reynolds numbers between 0.94 million and 3.7 million probably are small. The smaller lift-curve slope and the more forward location of the neutral point indicated by results from the 1- by 3-foot supersonic wind tunnel can be attributed partially to the effects of wing elasticity since the dynamic pressure during that investigation was approximately 50 percent greater than that of the present tests. Allowing for the difference in the elastic deformation effects, increasing Reynolds number from 0.94 million to 3.7 million at a Mach number of 1.53 appears to have little effect on lift-curve slope, drag-rise factor, minimum drag coefficient, maximum lift-drag ratio, and the location of the neutral point.

CONCLUSIONS

The results of a wind-tunnel investigation of a wing-body combination employing a wing with the leading edge swept back 63° and cambered and twisted to support a uniform load at a lift coefficient of 0.25 and a Mach number of 1.53 in the Ames 6- by 6-foot supersonic wind tunnel indicate the following:

1. A maximum lift-drag ratio of 8.9 and a minimum drag coefficient of 0.0145 was obtained at the design Mach number of 1.53.

2. The lift-curve slope decreased from 0.050 to 0.044 and the neutral pointed shifted from 57 percent of the mean aerodynamic chord rearward to 64 percent with increasing Mach number from 1.2 to 1.7.

3. Comparisons of the data with those obtained from an investigation of a geometrically similar model in a subsonic wind tunnel showed that the trend of the results conformed well with those obtained at subsonic speeds and comparable Reynolds number.

4. The results of an investigation of a geometrically similar model at a Mach number of 1.53 and a Reynolds number of 0.94 million compared well with those obtained during the present investigation, indicating little Reynolds number effect in the range of Reynolds numbers between 0.94 million and 3.7 million.

---

[4] In reference 5 the Reynolds number was 0.84 million based on the mean geometric chord. It is identical to a Reynolds number of 0.94 million based on the mean aerodynamic chord.

5. Comparisons of experimental results with theory indicated good agreement between the lift characteristics but less satisfactory agreement between the pitching-moment characteristics. Discrepancies were attributed primarily to differences between the experimental and theoretical chordwise loadings of the wing and to wing-fuselage interference effects.

Ames Aeronautical Laboratory,
National Advisory Committee for Aeronautics,
Moffett Field, Calif.,

REFERENCES

1. Jones, Robert T.: Estimated Lift-Drag Ratios at Supersonic Speeds. NACA TN 1350, 1947.

2. Madden, Robert T.: Aerodynamic Study of a Wing-Fuselage Combination Employing a Wing Swept Back 63°.- Characteristics at a Mach number of 1.53 Including Effect of Small Variations of Sweep. NACA RM A8J04, 1948.

3. McCormack, Gerald M., and Walling, Walter C.: Aerodynamic Study of a Wing-Fuselage Combination Employing a Wing Swept Back 63°.- Investigation of a Large-Scale Model at Low Speed. NACA RM A8D02, 1948.

4. Reynolds, Robert M., and Smith, Donald W.: Aerodynamic Study of a Wing-Fuselage Combination Employing a Wing Swept Back 63°.- Subsonic Mach and Reynolds Number Effects on the Characteristics of the Wing and on the Effectiveness of an Elevon. NACA RM A8D20, 1948.

5. Madden, Robert T.: Aerodynamic Study of a Wing-Fuselage Combination Employing a Wing Swept Back 63°.- Investigation at a Mach number of 1.53 to Determine the Effects of Cambering and Twisting the Wing for the Uniform Load at a Lift Coefficient of 0.25. NACA RM A9C07, 1949.

6. Jones, Lloyd and Demele, Fred: Aerodynamic Study of a Wing-Fuselage Combination Employing a Wing Swept Back 63°.- Characteristics Throughout the Subsonic Speed Range with the Wing Cambered and Twisted for a Uniform Load at a Lift Coefficient of 0.25. NACA RM A9D25, 1949.

7. Jones, Robert T.: Wing Plan Forms for High Speed Flight. NACA TN 1033, 1946.

8. Cohen, Doris: The Theoretical Lift of Flat Swept-Back Wings at Supersonic Speeds. NACA TN 1555, 1948.

9. Cohen, Doris: Theoretical Loading at Supersonic Speeds of Flat Swept-Back Wings with Interacting Trailing and Leading Edges. NACA TN 1991, 1949.

10. Betz A.: Applied Airfoil Theory. Vol. IV, div. J., sec. 1, ch. II of Aerodynamic Theory, W. F. Durand, ed., Julius Springer (Berlin), 1935.

11. Squire, H. B.: Theory of the Flow Over a Particular Wing in a Supersonic Stream. Rep. No. Aero 2184, R.A.E. (British), Feb.,1947.

12. Frick, C. W., and Chubb, R. S.: The Longitudinal Stability of Elastic Swept Wings at Supersonic Speed. NACA TN 1811, 1949.

13. Ribner, Herbert S., and Malvestuto, Frank S., Jr.: Stability Derivatives of Triangular Wings at Supersonic Speeds. NACA TN 1572, 1948.

14. Frick, C. W., and Olson, R. N.: Flow Studies in the Asymmetrical Adjustable Nozzle of the Ames 6- by 6-foot Supersonic Wind Tunnel. NACA RM A9E24, 1949.

15. Stevens, Victor I., and Boyd, John W.: A Comparison of Theoretical and Experimental Loading on a 63° Swept-Back Wing at Supersonic Speeds. NACA RM A9C16, 1949.

16. Haack, W.: Geschossformen Kleinsten Willenividerstandes. Lilienthal-Gesellschaft für Luftfahrtforschung, Bericht 39, Teil 1, pp. 14 - 28. (English Translation available from CADO, ATI 27736)

17. Perkins, Edward W.: Experimental Investigation of the Effects of Support Interference on the Drag of Bodies of Revolution at a Mach Number of 1.53. NACA RM A8B05, 1948.

18. Jones, Robert T.: Effects of Sweepback on Boundary Layer and Separation. NACA TN 1402, 1947.

19. Spreiter, John R.: Aerodynamic Properties of Slender Wing-Body Combinations at Subsonic, Transonic, and Supersonic Speeds. NACA TN 1662, 1948.

20. Myers, Boyd C., II, and King, Thomas J., Jr.: Aerodynamic Characteristics of a Wing with Quarter Chord Line Swept Back 45°, Aspect Ratio 4, Taper Ratio 0.3, NACA 65A006 Airfoil Section Transonic-Bump Method. NACA RM L9E25, 1949.

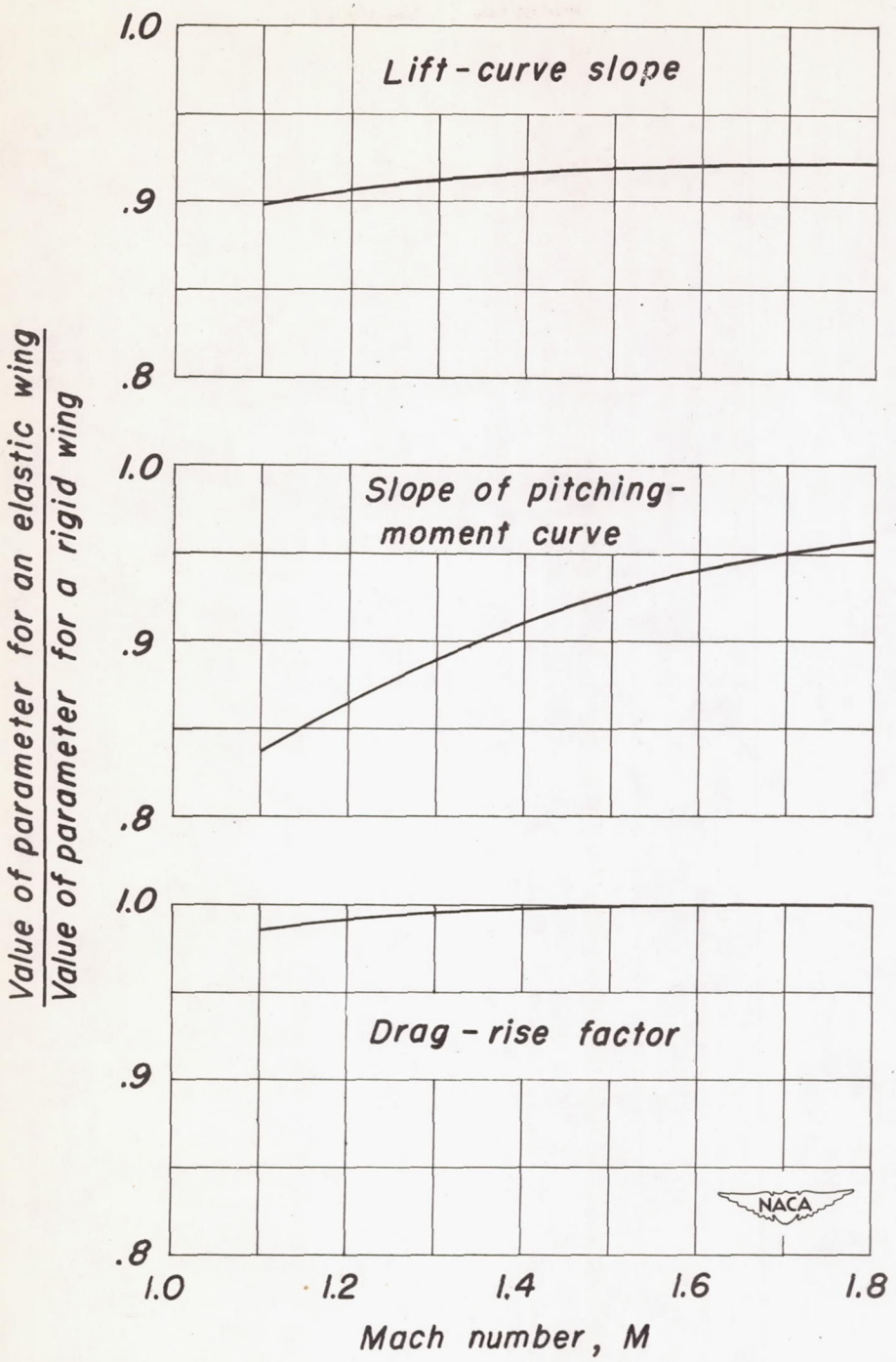

Figure 1.- The calculated effect of aeroelastic twist on the longitudinal characteristics of the twisted and cambered 63° swept-back wing model.

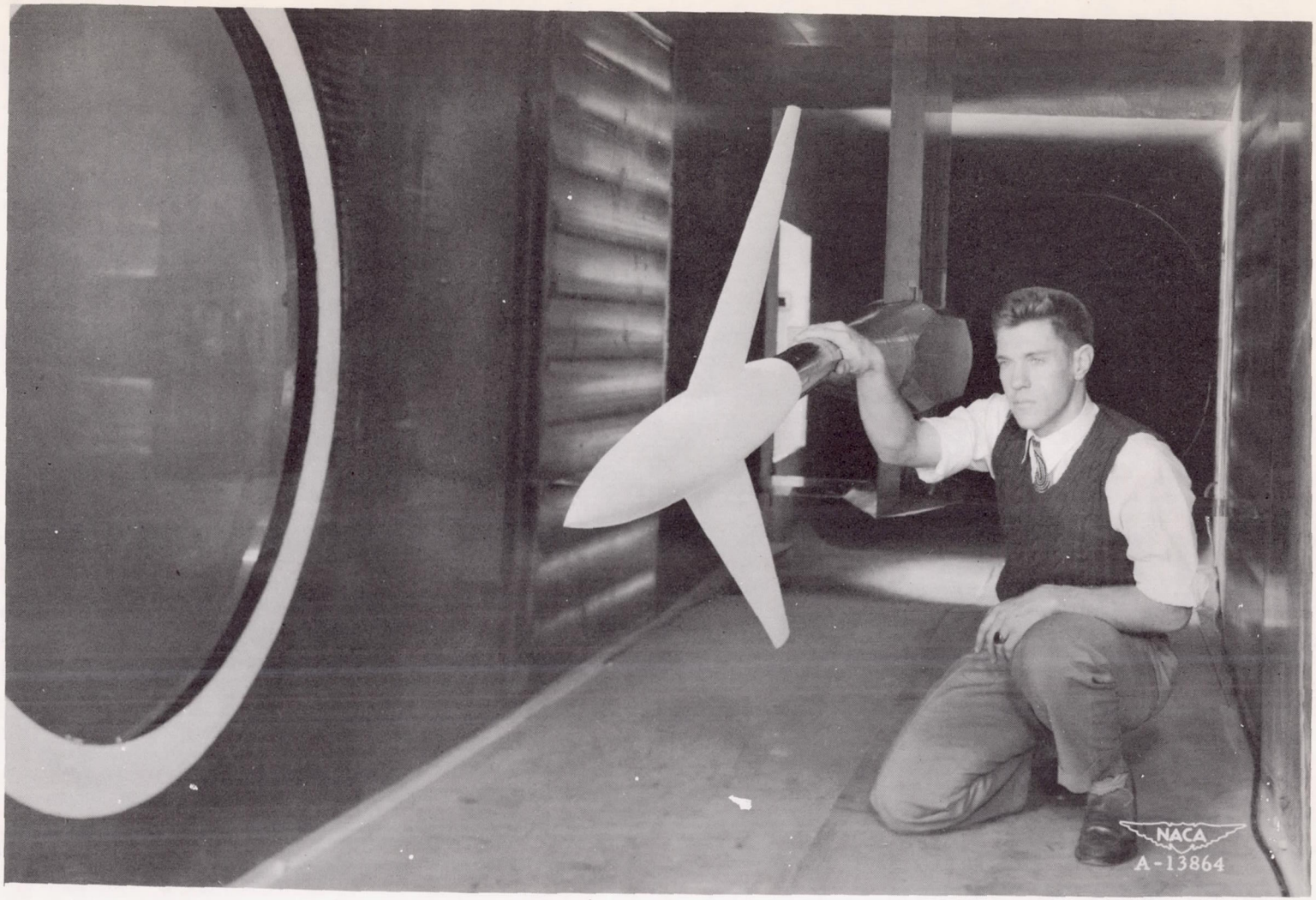

Figure 2.– The twisted and cambered 63° swept–wing model in the Ames 6– by 6–foot supersonic wind tunnel.

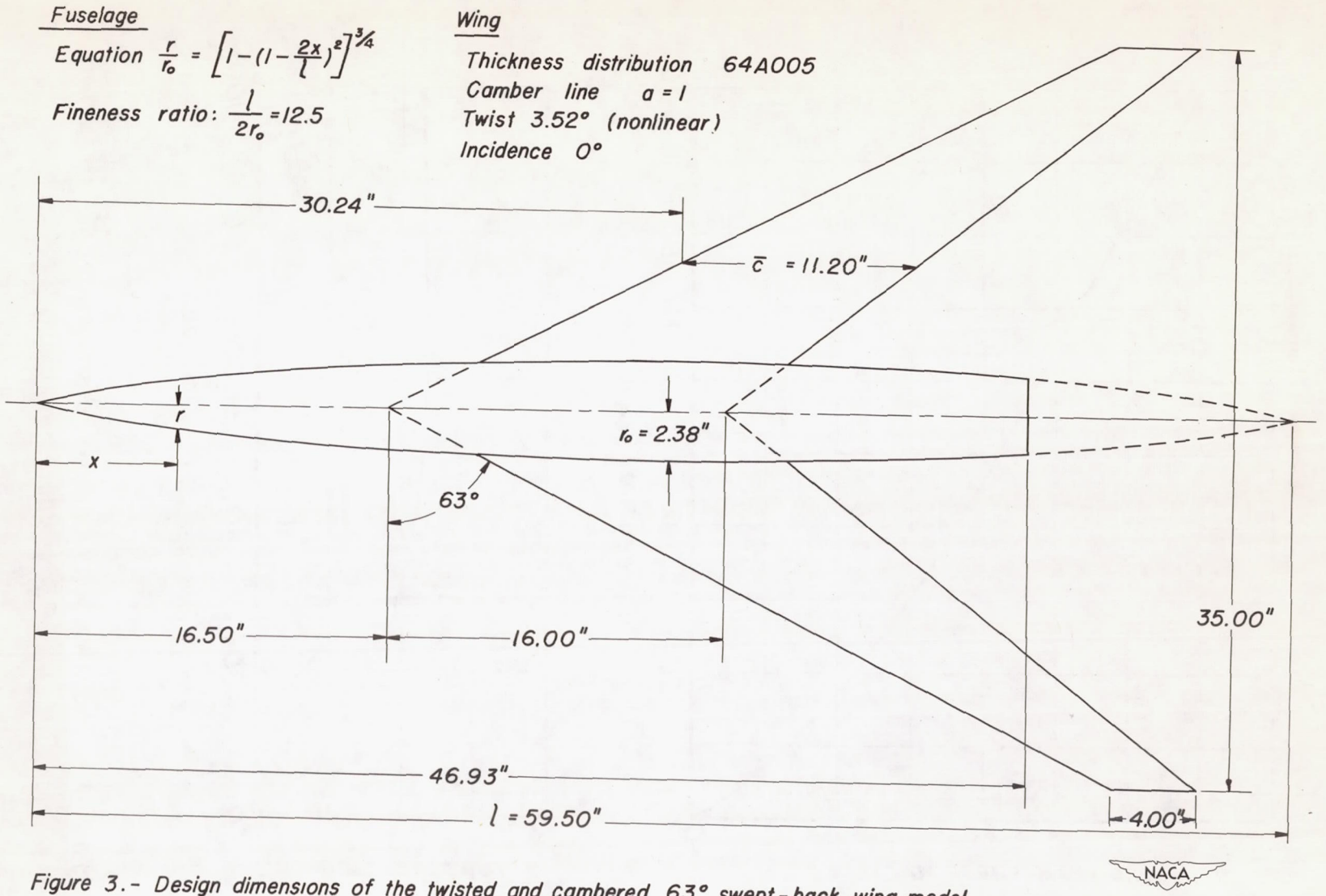

Figure 3.- Design dimensions of the twisted and cambered 63° swept-back wing model.

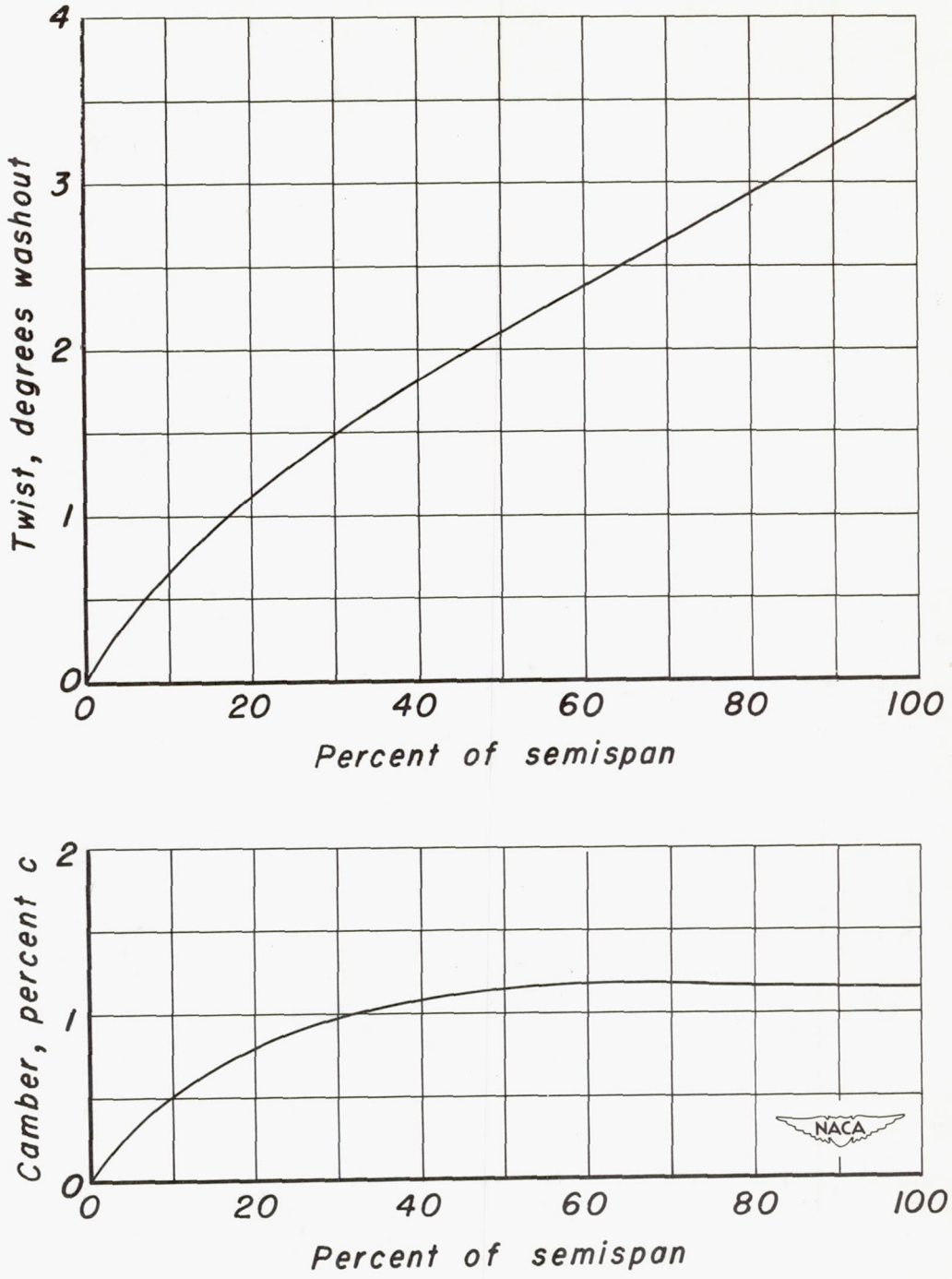

Figure 4.- The twist and camber distribution of streamwise sections of the 63° swept-back wing.

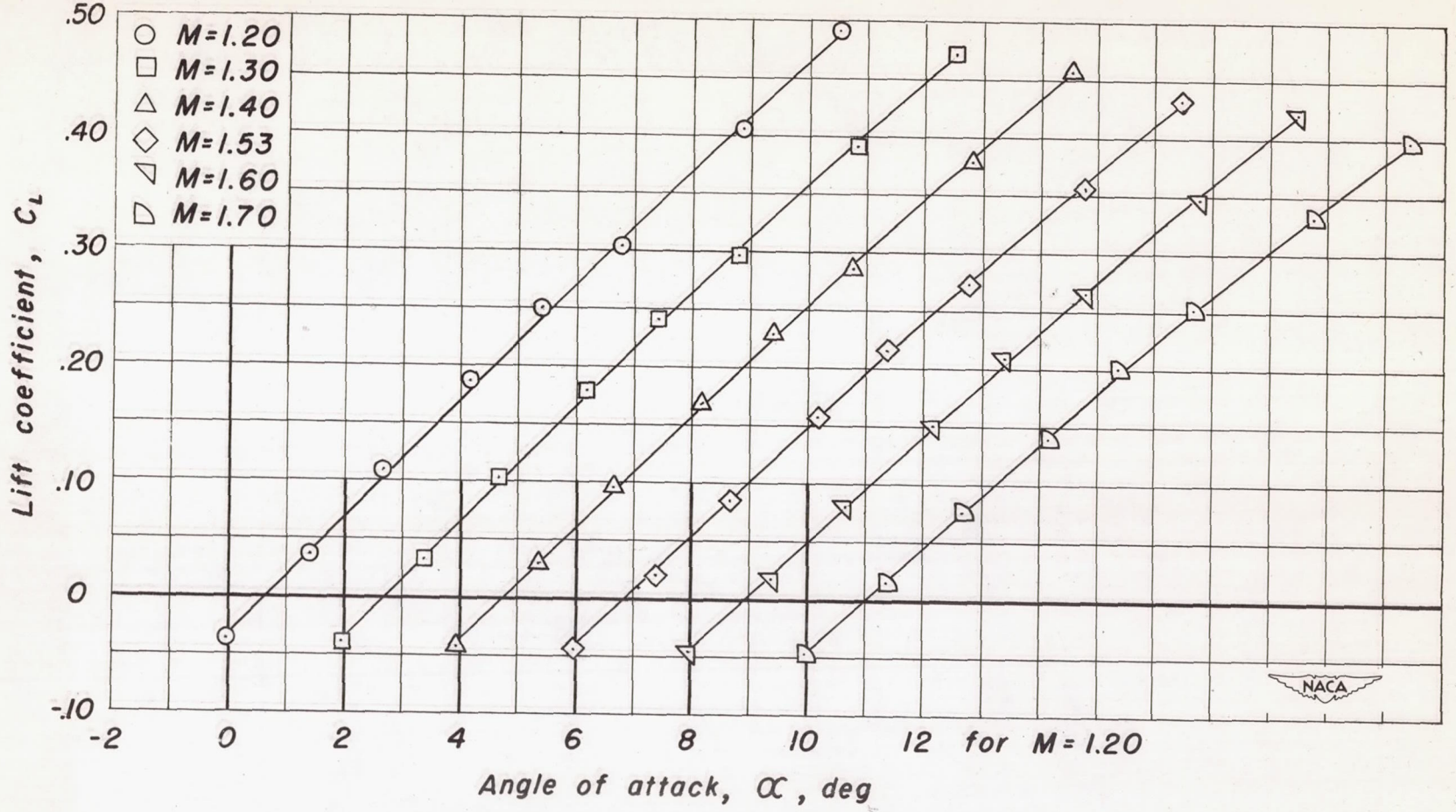

Figure 5.– The variation of lift coefficient with angle of attack for the twisted and cambered 63° swept-back wing model.

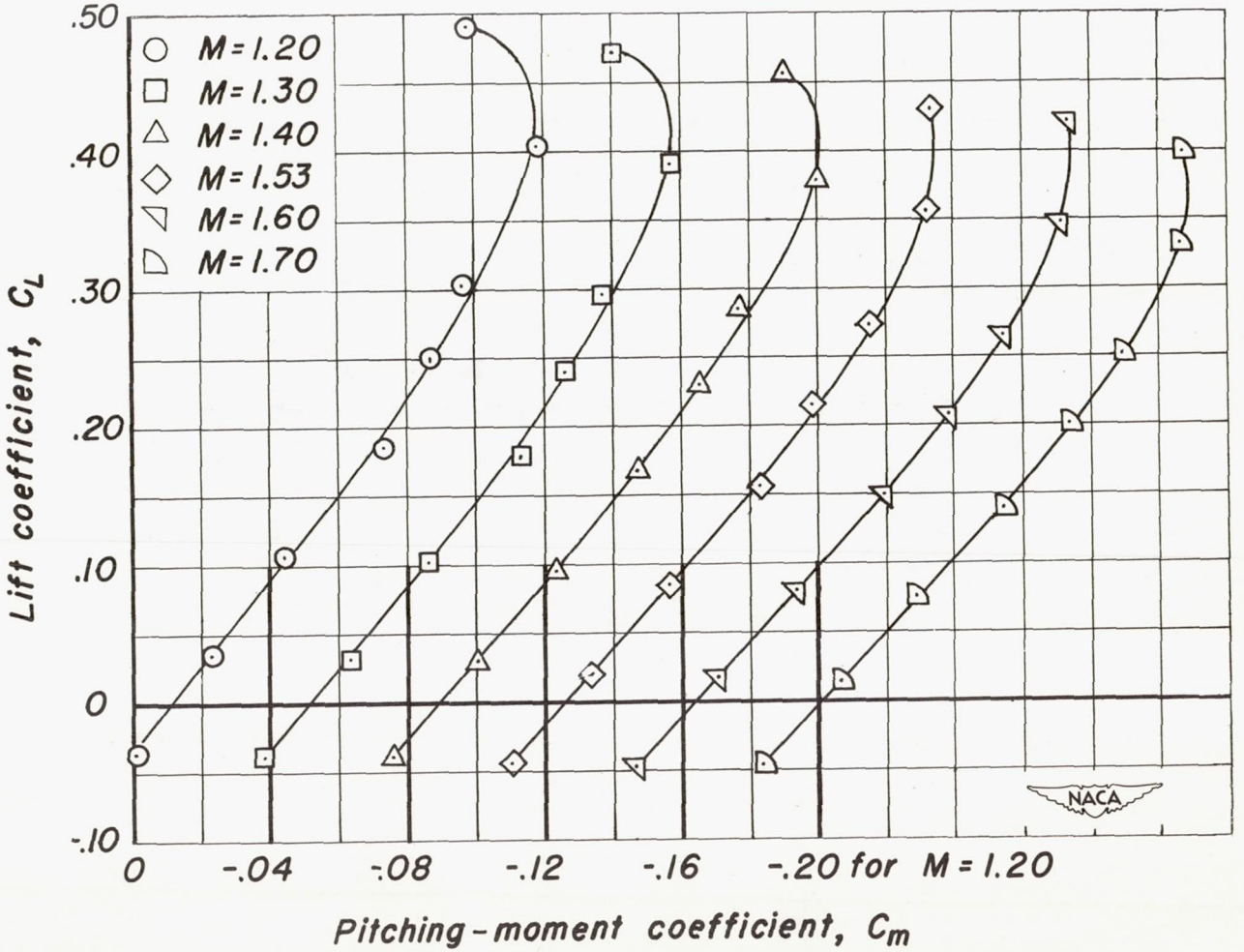

Figure 6.- The variation of pitching-moment coefficient with lift coefficient for the twisted and cambered 63° swept-back wing model.

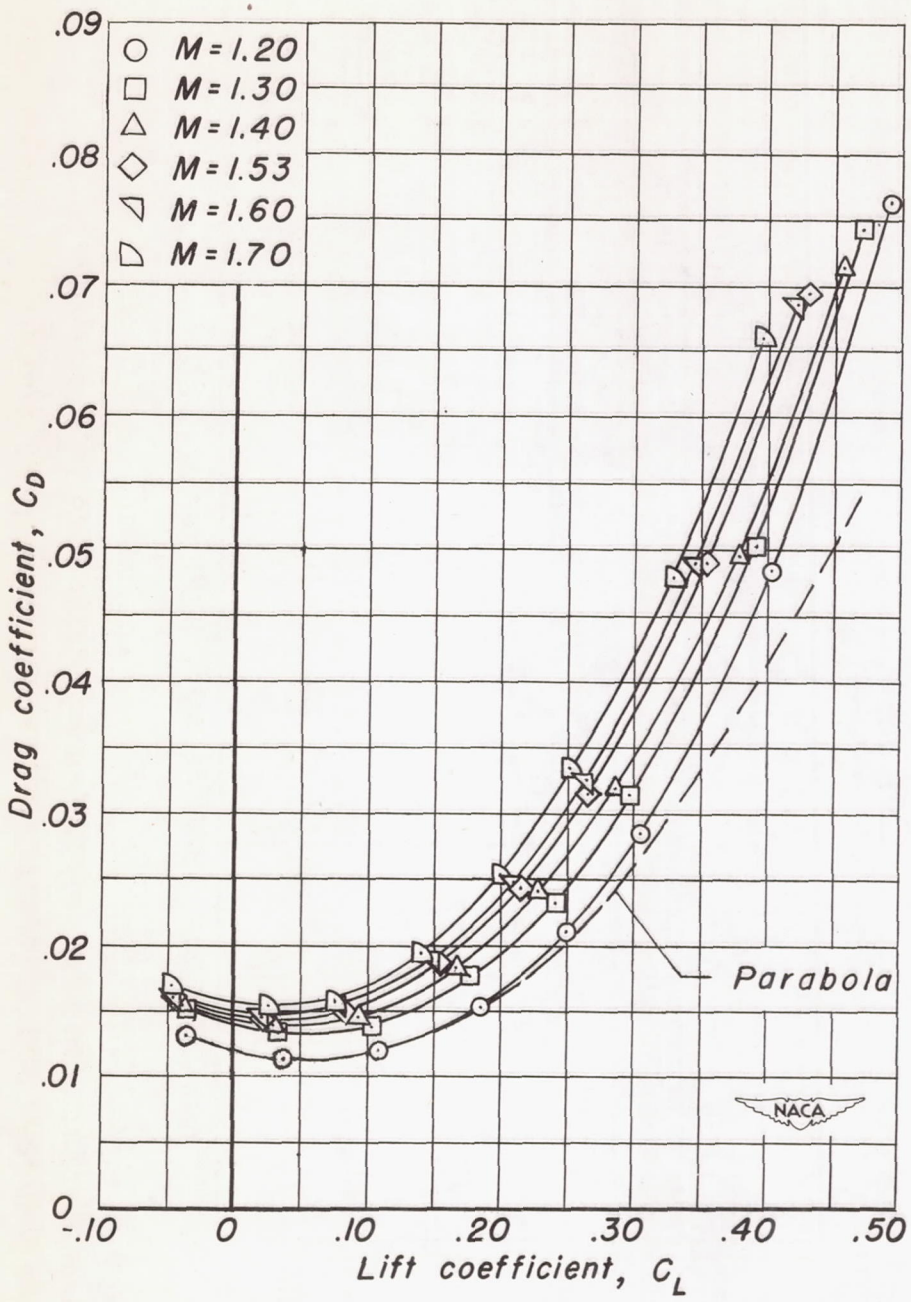

Figure 7.- The variation of drag coefficient with lift coefficient for the twisted and cambered 63° sweptback wing model.

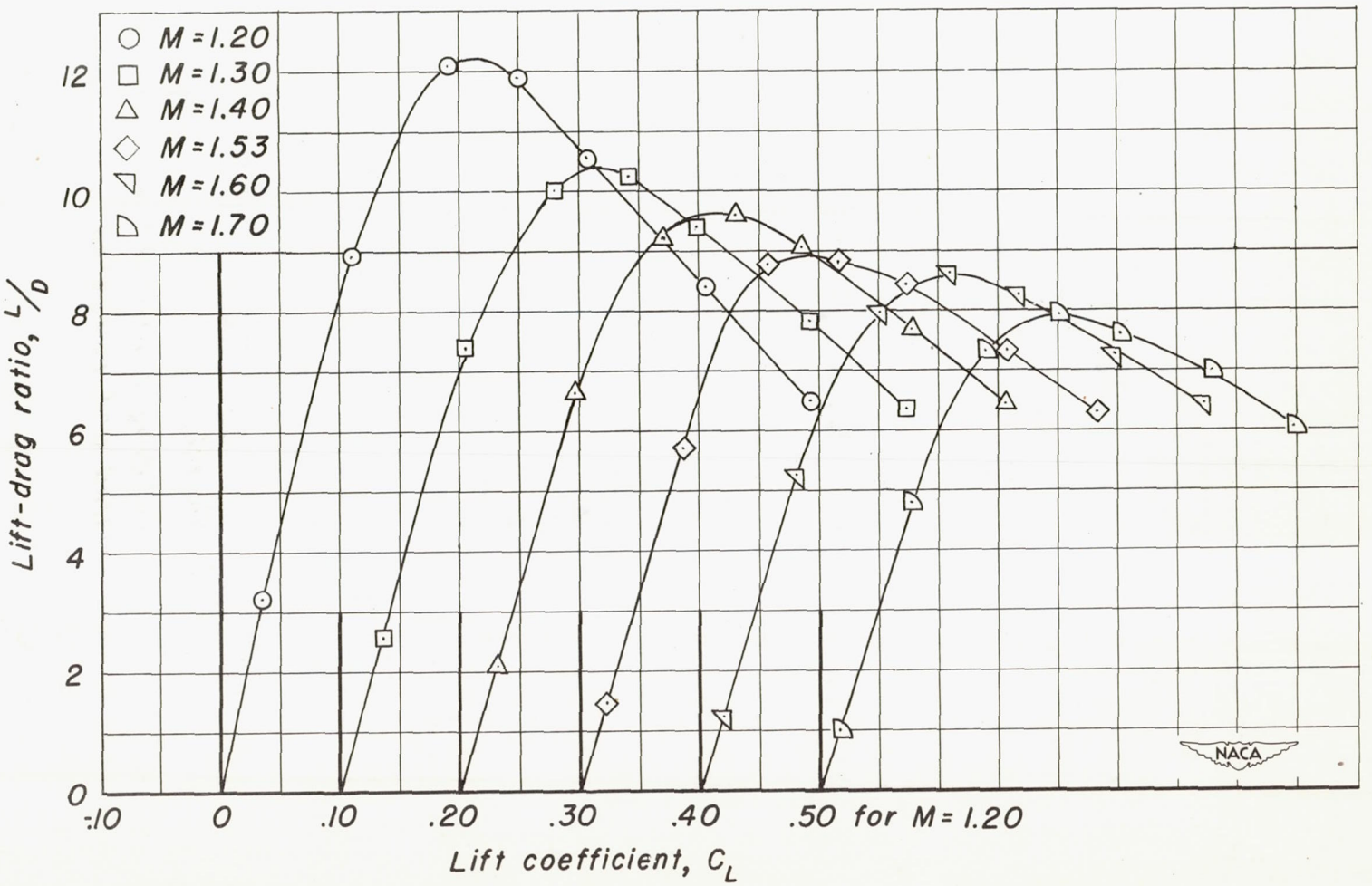

Figure 8.- The variation of lift-drag ratio with lift coefficient for the twisted and cambered 63° swept-back wing model.

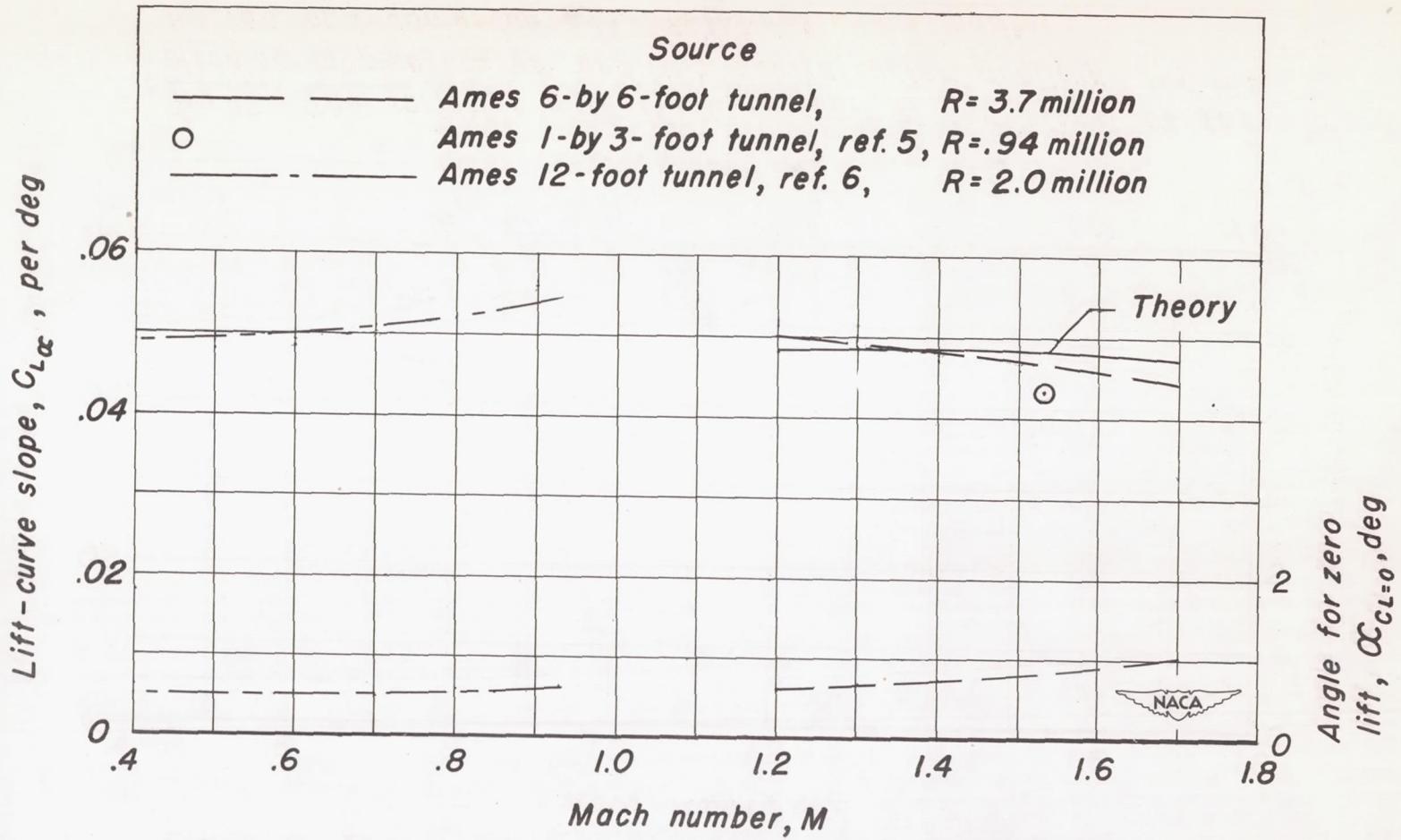

Figure 9.- The variation with Mach number of lift-curve slope and angle for zero lift for the twisted and cambered 63° swept-back wing model.

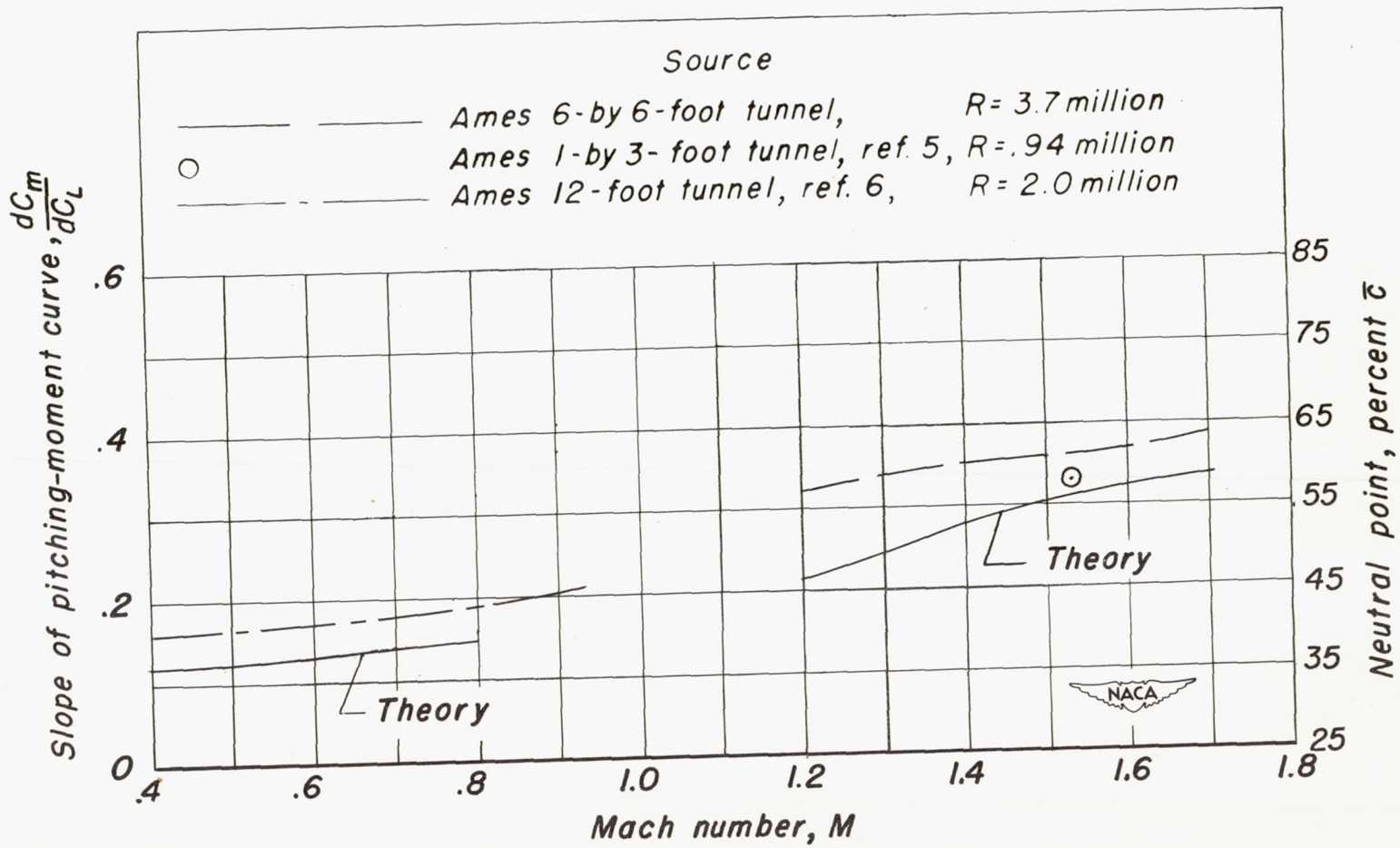

Figure 10.– The variation with Mach number of the slope of the pitching-moment curve and the neutral-point position for the twisted and cambered 63° swept-back wing model.

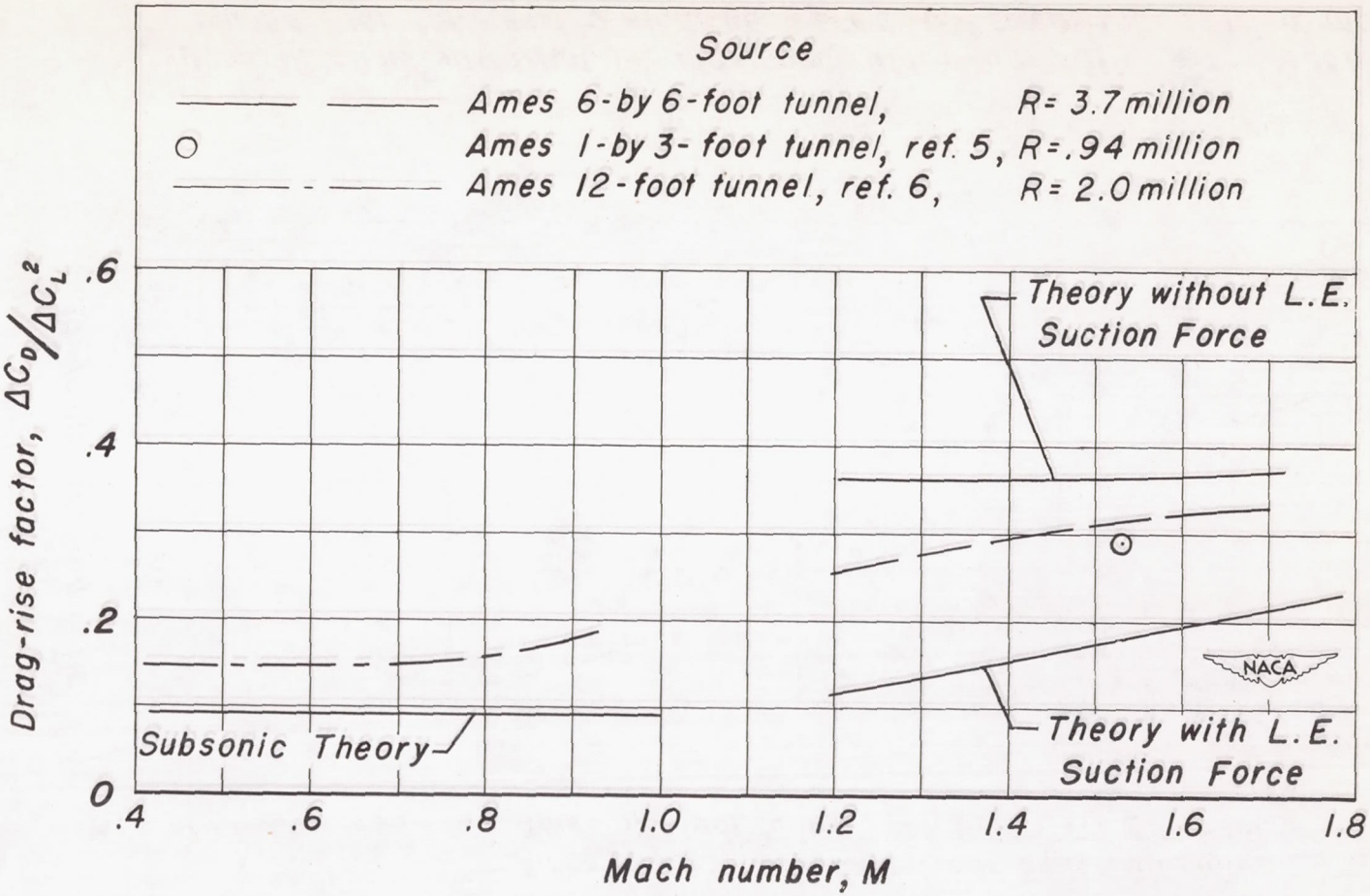

Figure 11.–The variation of the drag-rise factor with Mach number for the twisted and cambered 63° swept-back wing model.

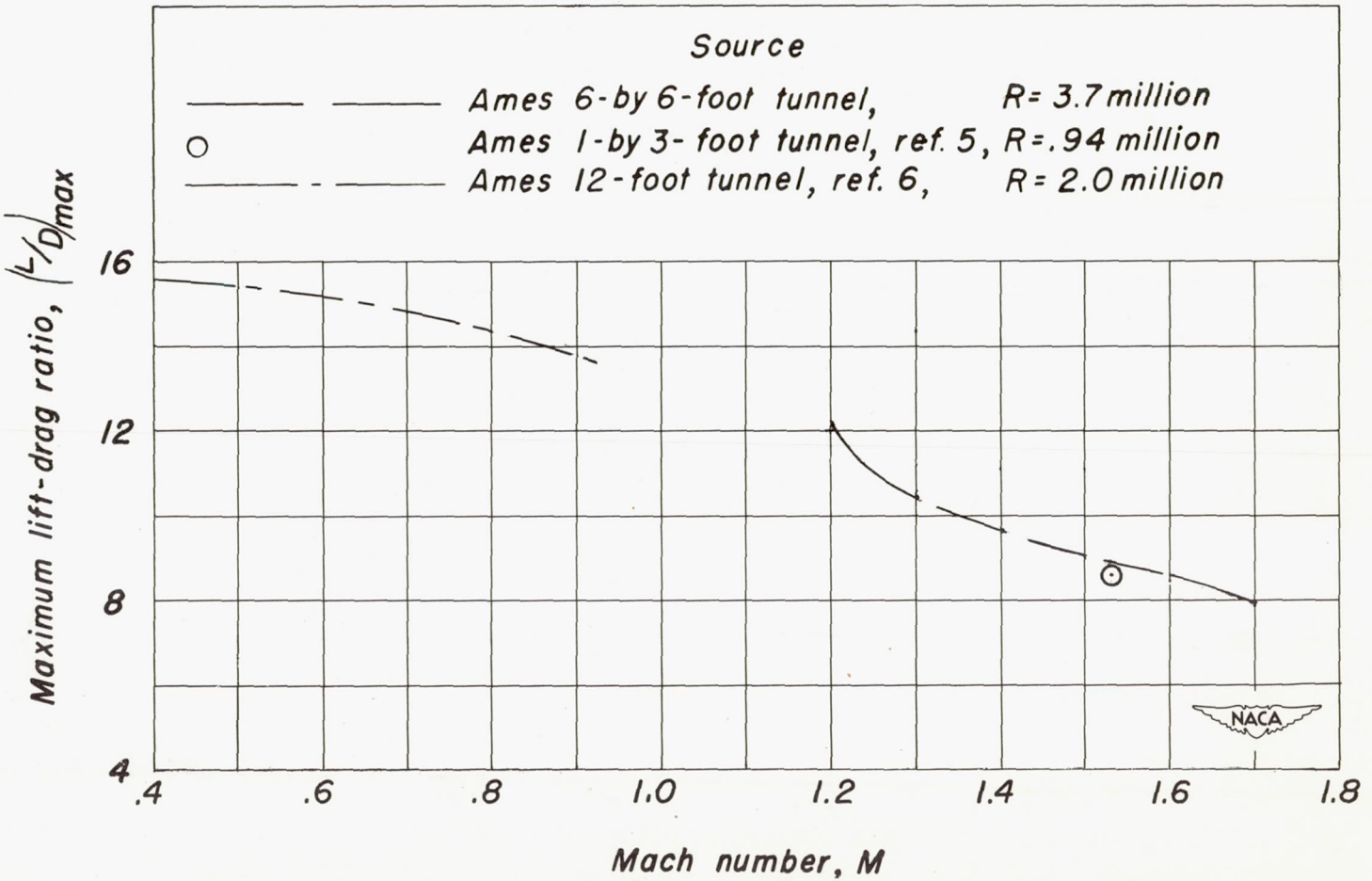

Figure 12.- The variation of maximum lift-drag ratio with Mach number for the twisted and cambered 63° swept-back wing model.

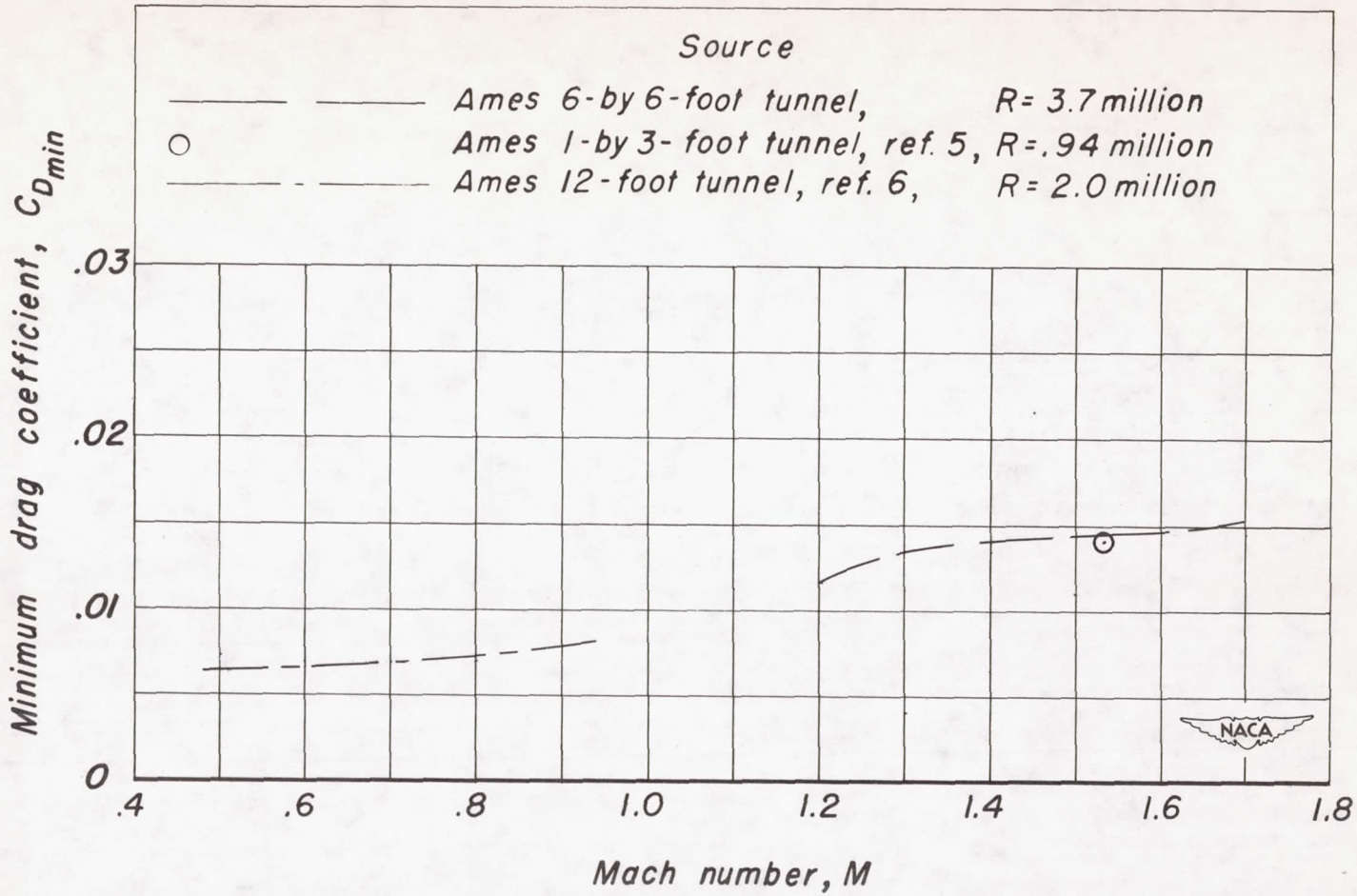

Figure 13.- The variation of minimum drag coefficient with Mach number for the twisted and cambered 63° swept-back wing model.